PROCEEDINGS OF SCIENCE

Test of the Tau and Muon Lepton Universality in W Boson Decays from $t\bar{t}$ events in ATLAS

Izaac Sanderswood*on behalf of the ATLAS collaboration

*Lancaster University,
Lancaster, United Kingdom

E-mail: izaac.sanderswood@cern.ch

The Standard Model of particle physics is our current best understanding of physics at the smallest scales. It assumes that, in the massless limit, the weak interactions of leptons are identical. This fundamental assumption is known as Lepton Flavour Universality (LFU) and can be tested by comparing the measured decay rates, or branching fractions (B), of (semi-)leptonic processes that differ only by lepton flavour. Such a test is summarised here, that compares the decay rates of W bosons to either τ-leptons or muons, using $R(\tau/\mu) = B(W \to \tau\nu)/B(W \to \mu\nu)$. The measurement is performed with a novel technique using di-leptonic $t\bar{t}$ events based on 139 fb^{-1} of proton-proton collision data at $\sqrt{s} = 13$ TeV recorded in the ATLAS detector at the LHC. τ-leptons are identifed through their decays to muons. The lifetime of the τ-leptons provides two distinguishing features to determine whether muons originate from the W boson decay or via intermediate τ-lepton: typically lower transverse momentum and a typically larger transverse impact parameter. The observed best-fit value of the ratio $R(\tau/\mu)$ is measured to be $0.992 \pm 0.013[\pm 0.007\ (\text{stat}) \pm 0.011\ (\text{syst})]$ which is in good agreement with the Standard Model expectation of unity. This result achieves an unprecedented precision which is particularly promising coming from a hadron collider.

BEAUTY2020
21-24 September 2020
Kashiwa, Japan (online)

*Speaker

PoS(BEAUTY2020)053

1. Introduction

The universality of the weak interactions of electrons (e), muons (μ) and τ-leptons (τ) is often considered a "sacred principle" of the Standard Model (SM) due to being well verified at low energies [1]. However, it is an *assumption* of the SM, rather than a requirement. Some results, for example from LEP [2] and recent "flavour anomalies" from b-factory experiments [3] show tension with SM predictions – a challenge to the assumption. These results could be hints of new physics that goes beyond the SM. Lepton Flavour Universality (LFU) is tested by comparing the measured decay rates, or branching fractions (B), of (semi-)leptonic processes that differ only by lepton flavour. These proceedings summarise such a test using the decays of on-shell W bosons that are produced in $t\bar{t}$ events, by measuring the ratio of branching ratios $R(\tau/\mu) = B(W \to \tau\nu)/B(W \to \mu\nu)$. A more detailed description is found in Ref. [4].

Previous tests of LFU using on-shell W bosons have provided tight constraints on universality between electrons and muons at the 1% level [5], agreeing with the SM assumption. This is not the case for tests using W boson decays to τ-leptons. The tightest constraint on $R(\tau/\mu)$ comes from the combined LEP result, which has a precision of 2.4% and is in agreement with the SM prediction of unity at the level of 2.7σ [2]. Therefore further tests are well motivated.

A large sample of top quark pairs ($t\bar{t}$) has been produced in the ATLAS detector [6] at the LHC [7] during Run-2. Being heavier than a W boson, the top quark decays semi-weakly, i.e. to an on-shell W boson and bottom quark, which occurs essentially 100% of the time. This means that the many $t\bar{t}$ decays in ATLAS's 139 fb^{-1} of pp collision data are an abundant source of on-shell W boson pairs that can be analysed to test LFU, using di-leptonic decay modes. These are used to measure the ratio of the decay rates of $t \to Wb \to \tau\nu b$ and $t \to Wb \to \mu\nu b$. The τ-leptons are identified through their decays to muons. This allows the measurement to take advantage of ATLAS's muon identification and reconstruction, which have lower uncertainties than for hadronically decaying τ-leptons. Another benefit is that many of the systematic uncertainties are correlated between the numerator and denominator in $R(\tau/\mu)$, and therefore mostly cancel. These include uncertainties related to jet reconstruction, flavour tagging and trigger efficiencies. Muons originating via intermediate τ-leptons are distinguished from the "prompt" muons originating in the W decays through the significant displacement of the τ-lepton decay vertex, and typically have a lower transverse momentum. The transverse impact parameter, $|d_0^\mu|$, is the closest approach of the muon track measured with respect to the luminous region in the x-y plane. A 2-D fit in $|d_0^\mu|$ and the transverse momentum, p_{T}^μ, is used to extract $R(\tau/\mu)$. In the SM, $R(\tau/\mu)$ is predicted to be unity down to the sub-per-mil level, at which point mass effects would need to be considered.

2. Event selection and calibration

A standard di-leptonic $t\bar{t}$ selection is applied, the details of which are described in Ref. [4]. The key requirements are exactly two oppositely charged leptons and at least 2 b-jets. Wt events that match these requirements are also treated as signal. The two leptons are exploited in a *tag* and *probe* approach: one of the leptons is used to trigger and *tag* the event, whilst the other is used to *probe* $R(\tau/\mu)$. This approach provides a sample of *probe* muons with unbiased p_{T}^μ and $|d_0^\mu|$ distributions, and since only the *tag* lepton is required to have a high enough p_{T} to trigger the event, the *probe*

can have a much lower p_{T}^{μ}, down to 5 GeV. Details of the data and Monte Carlo simulation samples are provided in Ref. [4]. The *tag* lepton is used to trigger the event and can be either a muon or an electron. The *probe* lepton must be a muon. This results in two channels according to *tag* and *probe*: e-μ and μ-μ. In the μ-μ channel, both muons can satisfy *tag* and *probe* requirements. In this case, both are used as *probe* muons. This eliminates any bias in the p_{T}^{μ} of the *probe* muons. To minimise contributions from Drell-Yann $Z(\rightarrow \mu\mu)$ + jets, a Z veto is applied in the μ-μ channel.

The selection results in a high-purity $t\bar{t}$ (and Wt) sample. There are small backgrounds where the *probe* muon originates either from non-prompt hadron decays or prompt (non-top) decays.

2.1 Monte Carlo Calibration

The measurement of $R(\tau/\mu)$ is sensitive to the accuracy of the simulation of the $|d_0^{\mu}|$ distributions. To improve the simulation of the detector, the $|d_0^{\mu}|$ shapes, or templates, of prompt muons (μ_{prompt}) and the $|d_0^{\mu}|$ resolutions of muons produced via intermediate taus ($\mu_{\tau(\rightarrow\mu)}$) and hadron decays ($\mu_{\mathrm{had.}}$) are all predicted using a $Z \rightarrow \mu\mu$ calibration region.

The calibration region is defined by modifying the nominal selection in two ways. First, the invariant mass of the two muons is required to be in the Z peak region $85 < M(\mu\mu) < 100$ GeV. Second, the hadronic jet requirements are dropped. This gives a large, pure sample of prompt muons produced from Z decays. The calibration region is divided into 33 kinematic bins of η and p_{T}^{μ}, which captures the dependence of the $|d_0^{\mu}|$ distributions on these variables. The templates are derived separately in different data-taking periods to account for differences in the beam conditions and alignment of the inner detector.

The μ_{prompt} templates are derived in each of the kinematic bins by taking the $|d_0^{\mu}|$ shape from the calibration region and scaling it to the number of events in the signal region, after subtracting expected background contributions.

For muons with significant displacement, smearing is applied to correct the resolution in simulation to what is measured in data. The resolution of the $\mu_{\tau(\rightarrow\mu)}$ and $\mu_{\mathrm{had.}}$ components is measured in each kinematic bin in the calibration region. The $|d_0^{\mu}|$ distributions are approximated as Gaussian distributions by fitting such a curve in the range $0 < |d_0^{\mu}| < 0.02$ mm, after subtracting estimated non-prompt contributions. For the range of $|d_0^{\mu}|$ values considered in this analysis, the resolution measured from prompt muons is applicable to those with significant displacement.

3. Backgrounds

The event selection provides a high purity di-leptonic $t\bar{t}$ (and Wt) sample. The main backgrounds are from muons that originate from hadron decays ($\mu_{\mathrm{had.}}$) in both the e-μ and μ-μ channels, and Drell-Yann $Z(\rightarrow \mu\mu)$ + jets in the μ-μ channel only. The scale factors for these backgrounds are estimated in distinct control regions and applied to the signal region in the fit to extract $R(\tau/\mu)$.

The $\mu_{\mathrm{had.}}$ background is important at high values of $|d_0^{\mu}|$ and low values of p_{T}^{μ}, where it occurs in the same phase space as $\mu_{\tau(\rightarrow\mu)}$. Scale factors for this background are calculated using a same-sign control region in each channel. The $\mu_{\mathrm{had.}}$ component dominates this region, but has a similar size as in the signal region. In contrast to the signal region, the control regions require same-sign lepton pairs. The scale factors are estimated in these control regions by comparing the numbers of $\mu_{\mathrm{had.}}$ events in data and simulation, after correcting and subtracting the estimated contributions

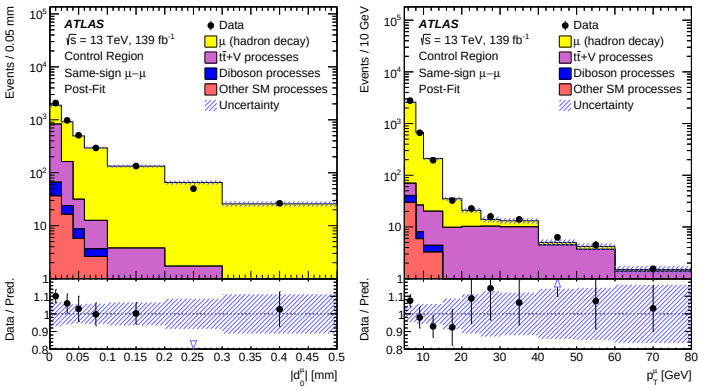

Figure 1: The $|d_0^\mu|$ (left) and p_{T}^μ (right) distributions in the same-sign control region for the μ-μ channel. The calculated scale factors have been applied. Good agreement between data and simulation is observed. As shown in Ref. [4].

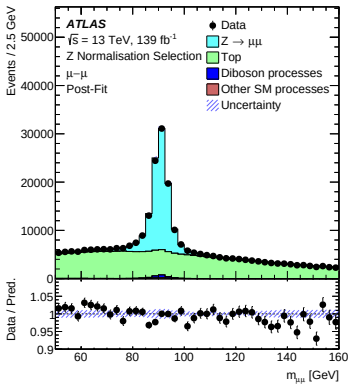

Figure 2: The di-muon invariant mass distribution in the $Z(\rightarrow \mu\mu)$ + jets control region, used to determine the background scale factor. As shown in Ref. [4].

from other sources (such as $t\bar{t} + V$ and diboson processes). Simulation is used to extrapolate from the control regions to the signal regions, as well as for the shape of the $|d_0^\mu|$ distributions. Figure 1 shows the agreement between data and prediction. Good agreement is seen which gives confidence in the modelling of the $|d_0^\mu|$ and p_{T}^μ distributions for $\mu_{\mathrm{had.}}$. The main uncertainties from this approach are due to the limited statistics in the control regions, with small uncertainty due to the correction applied to other processes that are subtracted.

The μ-μ channel also sees significant background at low values of $|d_0^\mu|$ from Drell-Yann $Z(\rightarrow \mu\mu)$ + jets production. The scale factor for this process is obtained using data in a control region, which is defined by removing the Z-veto criterium of the signal region. The invariant mass distribution of the di-muon pair in this control region is fitted in the range $50 < m_{\mu\mu} < 140$ GeV. The fit uses a composite of a Voigt profile (a convolution of a Breit Wigner and a Gaussian) for the $Z \rightarrow \mu\mu$ resonance, and a 3rd-order Chebychev polynomial for all non-resonant processes. Figure 2 shows the control region after the derived scale factor has been applied, and shows good agreement between data and prediction. The systematic uncertainty of this is estimated by using different fitting functions.

4. Profile likelihood fit setup and systematic uncertainties

A 2-D profile likelihood fit [8] in bins of $|d_0^\mu|$ and p_{T}^μ is used in order to extract $R(\tau/\mu)$. The bin boundaries were selected to provide significantly differing contributions of μ_{prompt}, $\mu_{\tau(\rightarrow\mu)}$ and $\mu_{\mathrm{had.}}$. Optimisation resulted in three bins in p_{T}^μ (with boundaries of (5, 10, 20, 250 GeV), and eight bins in $|d_0^\mu|$ (with boundaries of 0, 0.01, 0.02, 0.03, 0.04, 0.06, 0.09, 0.15, 0.5 mm), in each of the e-μ and μ-μ channels.

The fit is setup with two floating parameters: $k(t\bar{t})$ and the parameter of interest $R(\tau/\mu)$. $k(t\bar{t})$ is the ratio of the normalisation of both the μ_{prompt} and $\mu_{\tau(\rightarrow\mu)}$ components of the $t\bar{t}$ and Wt processes to the total predicted events (using the theoretical cross sections). $R(\tau/\mu)$ only affects the $\mu_{\tau(\rightarrow\mu)}$

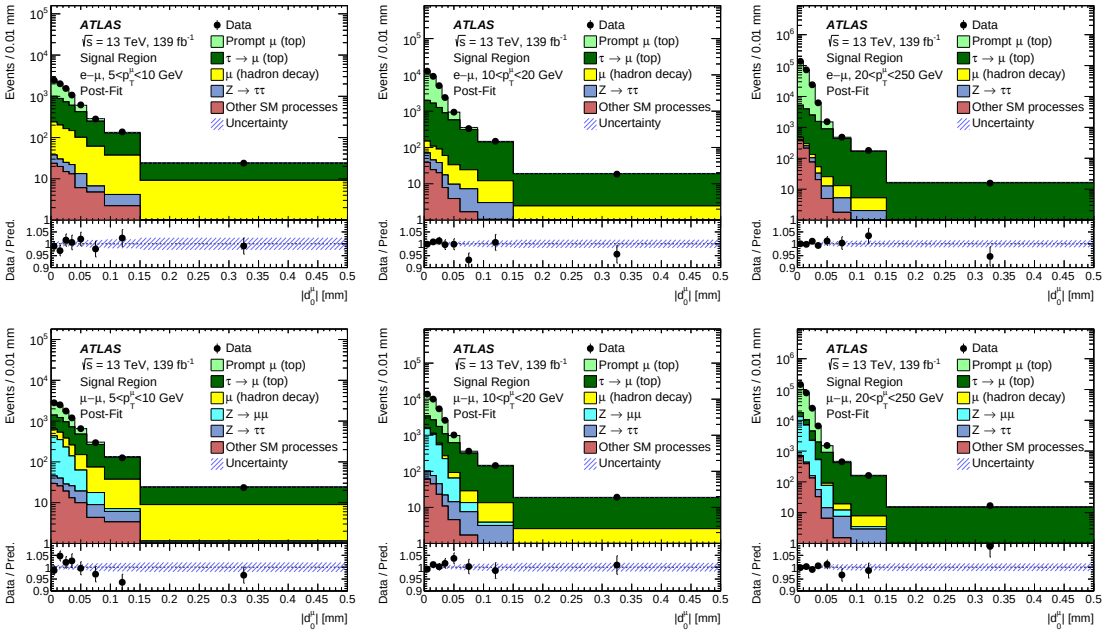

Figure 3: The post-fit $|d_0^{\mu}|$ distributions in each of the different p_{T}^{μ} bins, for e-μ (top) and μ-μ (bottom). As shown in Ref. [4].

components. It therefore controls the relative contributions of the μ_{prompt} and $\mu_{\tau(\to\mu)}$ templates – it is the ratio of the two. The scale factors with 1σ uncertainties for the main backgrounds are derived as described above and implemented as nuisance parameters in the fit. All other background processes are normalised to their higher order cross-sections and treated as nuisance parameters with 1σ uncertainties given by the uncertainty on these cross-sections.

The full details of the dominant systematic uncertainties and their estimation is provided in Ref. [4], but they can be summarised as follows:

- Uncertainties on the predicted templates for the μ_{prompt} components: These are estimated from the full difference between the templates from Z and $t\bar{t}$ in simulation.
- Top quark modelling uncertainties: These are estimated by comparing various Monte Carlo generator configurations.
- Muon identification and reconstruction uncertainties: These are estimated in dimuon ($Z \to \mu\mu$ and $J/\psi \to \mu\mu$) data and MC using a tag and probe method [9].
- Background ($\mu_{\text{had.}}$) scale factor uncertainties: These are estimated as described in Section 3.

5. Results

To avoid experimenter-expectancy bias, the analysis was developed blind to the central value on $R(\tau/\mu)$. All inputs to the fit were finalised before unblinding. The robustness of the result was further ensured by separately extracting $R(\tau/\mu)$ in various sub-regions.

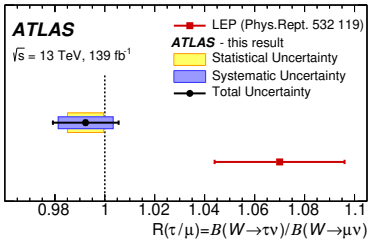

Figure 4: The observed best fit value of $R(\tau/\mu)$, shown alongside the previous LEP result. As shown in Ref. [4].

Figure 3 shows the post fit $|d_0^{\mu}|$ distributions in each of the three p_{T}^{μ} bins. The differing μ_{prompt}, $\mu_{\tau(\to\mu)}$ and $\mu_{\mathrm{had.}}$ contributions can be seen in each of the p_{T}^{μ} bins. Very good agreement between data and prediction is seen. The observed best fit value of $R(\tau/\mu)$ is:

$$R(\tau/\mu) = 0.992 \pm 0.013[\pm 0.007\ (\mathrm{stat}) \pm 0.011\ (\mathrm{syst})]$$

which is in agreement with the Standard Model assumption of unity and therefore supports the assumption of the universality of lepton interactions. The result is shown alongside the combined LEP measurement in Figure 4. The result presented here differs from the LEP result, which showed some tension with the Standard Model. This result achieves an unprecedented precision which is particularly impressive coming from a hadron collider.

References

[1] A. Pich, *Precision Tau Physics*, *Prog. Part. Nucl. Phys.* **75** (2014) 41 [1310.7922].

[2] ALEPH, DELPHI, L3, OPAL, LEP Electroweak collaboration, *Electroweak Measurements in Electron-Positron Collisions at W-Boson-Pair Energies at LEP*, *Phys. Rept.* **532** (2013) 119 [1302.3415].

[3] G. Ciezarek, M. Franco Sevilla, B. Hamilton, R. Kowalewski, T. Kuhr, V. Lüth et al., *A Challenge to Lepton Universality in B Meson Decays*, *Nature* **546** (2017) 227 [1703.01766].

[4] ATLAS collaboration, *Test of the universality of τ and μ lepton couplings in W-boson decays from $t\bar{t}$ events with the ATLAS detector*, 2007.14040.

[5] Particle Data Group collaboration, *Review of Particle Physics*, *PTEP* **2020** (2020) 083C01.

[6] ATLAS collaboration, *The ATLAS Experiment at the CERN Large Hadron Collider*, *JINST* **3** (2008) S08003.

[7] L. Evans and P. Bryant, eds., *LHC Machine*, *JINST* **3** (2008) S08001.

[8] G. Cowan, K. Cranmer, E. Gross and O. Vitells, *Asymptotic formulae for likelihood-based tests of new physics*, *Eur. Phys. J. C* **71** (2011) 1554 [1007.1727].

[9] ATLAS collaboration, *Muon reconstruction performance of the ATLAS detector in proton–proton collision data at $\sqrt{s}$ =13 TeV*, *Eur. Phys. J. C* **76** (2016) 292 [1603.05598].